RECENT ADVANCES IN THE QUANTITATIVE UNDERSTANDING OF FRICTION STIR WELDING

A. DE[1] and **T. DEBROY**[2]
[1]Indian Institute of Technology, Bombay, India
[2]The Pennsylvania State University, University Park, PA, USA. E-mail: amit@iitb.ac.in

Friction stir welding (FSW) is a relatively new welding process and its comprehensive understanding is still developing. While the process is commercially used for aluminum and other soft alloys, its commercial application for the welding of hard alloys will require development of cost-effective and durable tools. Here we review the recent progress made in numerical modeling heat transfer and material flow with particular emphasis on optimizing tool dimensions and selection of welding conditions for maximizing tool durability. 22 Ref., 2 Tables, 6 Figures.

Keywords: *friction stir welding, numerical modeling, heat transfer, material flow, welding conditions, tool durability*

In the last two decades, the applications of friction stir welding (FSW) in aerospace, shipbuilding, transportation and other industries have grown significantly, particularly for the welding of aluminum and other soft alloys [1–3]. General reviews of the FSW process are available in the literature [1–3]. Because melting of the parts is avoided, the process offers several important benefits compared to the conventional fusion welding processes. As a result, there is considerable commercial interest in the friction stir welding of steels and other hard alloys [4–6]. The FSW process involves several simultaneous physical phenomena that affect the durability of the tool and the structure and properties of the welded material. Heat is generated due to both the interfacial friction between the tool and the work piece and the plastic deformation of work piece material. The work piece material is softened close to the tool and the plasticized material flows due to rotation and the linear movement of the tool.

FSW is a relatively new process, and because of the complexity of the process a comprehensive understanding of the process is still evolving [7–13]. Therefore, it is useful to undertake a review of the current status of quantitative understanding of the process. Here we review our recent research on numerical modeling of heat transfer and material flow in FSW and how it can be used for the solution of two important contemporary problems. First, the application of the heat transfer and material flow model to estimate the optimum tool dimensions is discussed. Second, we show that the model can be used to enhance longevity of the FSW tools, particularly for the welding of hard alloys.

Optimum shoulder diameter. The diameter of the tool shoulder is important because the shoulder generates most of the heat, and its grip on the plasticized material largely establishes the material flow field [14–15]. Both the heat generation rate and the material flow are important for the FSW process. With the increase in the shoulder diameter, the temperature increases and the work piece material is softened. For a good FSW practice, the material should be adequately softened for flow, the tool should have adequate grip on the plasticized material, and the total torque and power should not be excessive [15]. Experimental investigations have shown that only a tool with an optimal shoulder diameter results in the highest strength of the AA6061 FSW joints [16]. Although the need to determine an optimum shoulder diameter has been recognized in the literature, the search for an appropriate principle for the determination of an optimum shoulder diameter is just beginning [14–15].

We recently proposed [14, 15] a method to determine the optimal shoulder diameter for the FSW of aluminum alloys by considering the sticking (M_T) and sliding (M_L) components of torque. The main engine for the calculations is a steady three dimensional heat transfer and material flow model which was validated for friction stir welding of aluminum alloys, steels and a titanium alloy [7, 8, 10]. The torques were calculated based on the tool geometry, flow stresses in work piece, and the axial pressure (PN) as [14, 15]

$$M_T = \oint_A r_A(1 - \delta)\tau dA, \quad (1)$$

$$M_L = \oint_A r_A \delta \mu_f P_N dA, \quad (2)$$

where r_A is the distance of any infinitesimal area element, dA, in work piece material from the tool axis; d and m_f are spatially variable fractional slip and coefficient of friction between the tool and the work piece, respectively, and t is the shear stress at yielding. The tool rotation speed and the radial distance from tool axis affect the local values of d and m_f [14, 15]. The total torque, M is the sum of sticking and sliding torques. The required spindle power (P) can be calculated from the total torque as [14]

$$P = \int_A r_A\{(1 - \delta)\tau + \delta\mu_f P_N\}\omega r_A dA, \qquad (3)$$

where ω refers to the angular speed in rad/s.

Figure 1 shows that for the FSW of AA6061, the sliding torque continuously increases with shoulder diameter because of the larger tool-work piece interfacial area. However, the sticking torque increases, reaches a maximum and then decreases. This behavior can be understood from equation (1) that includes the two important factors that affect the sticking torque. First, with the increase in shoulder diameterthe area, A, increases, the temperature rises and the shear stress at yielding, t, decreases. The product of these two opposing factors lead to a maximum value of sticking torque in the plot of sticking torque versus shoulder diameter. This value of sticking torque indicates the maximum grip of the shoulder on the plasticized material [14, 15]. The calculated results show that any further increase in the shoulder diameter will result in decreased grip of the tool on the plasticized material, higher total torque and higher spindle power requirement. For these reasons, the optimum shoulder diameter should correspond to the maximum sticking torque for a given set of welding parameters and work piece material [14, 15].

Figure 2 shows the variation of sticking torque with shoulder diameter for various tool rotational speeds for the FSW of 7075 aluminum alloy. The shoulder diameter at which the maximum sticking torque is attained depends on tool rotational speedwhenall other welding variables aremaintained constant. For the rotational speeds indicated in the figure, the optimum values of the shoulder diameter are in the 20 to 30 mm range for the various parameters used in the experiments. Since the 7075 alloy is harder than the 6061 aluminum alloy, the computed larger optimum shoulder diameters compared with those estimated for the FSW of 6061 is consistent with the larger heat demand for the FSW of 7075 alloy. The results show that the principle of optimizing shoulder diameter by maximizing tool's grip on the plasticized material can be applied to different alloys. Since tool durability and cost-effectiveness are crucial issues for successful commercial application of

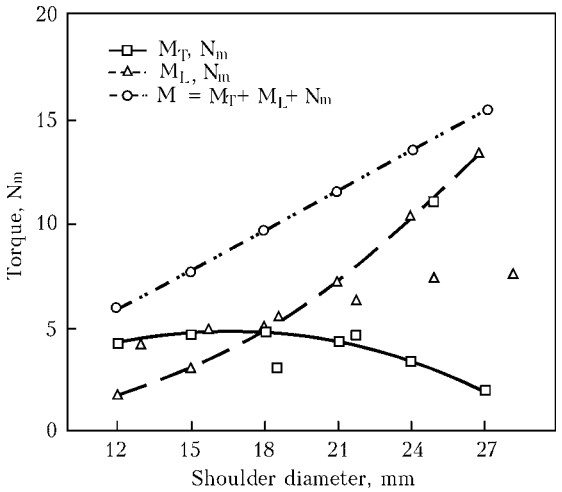

Figure 1. Variation in sliding (M_L), sticking (M_T) and total torques with shoulder diameter for FSW of 6 mm thick AA6061 at a tool rotational speed of 1200 rpm and welding speed of 1.25 mm/s^{-1} [15]

FSW to steels and other hard alloys, a general principle for the optimum design of shoulder diameter based on scientific principle such as the one discussed here is important.

Pin geometry. Since tool pins often fail during welding of hard alloys, a systematic investigation of the various tool materials and their load-bearing abilities are important [17]. In particular, the pin being the structurally weakest section of the FSW tool, an estimation of the load bearing ability of the tool pin is required for efficient functioning of the FSW process. Although some measurements and calculations of the forces on the tool have been reported in the literature, a procedure to calculate the load bearing ability of the tool pins of different shapes is of interest [18, 19]. Such a methodology has beendiscussedrecently based on the calculation of maximum stresses experienced by the tool pin resulting from a combi-

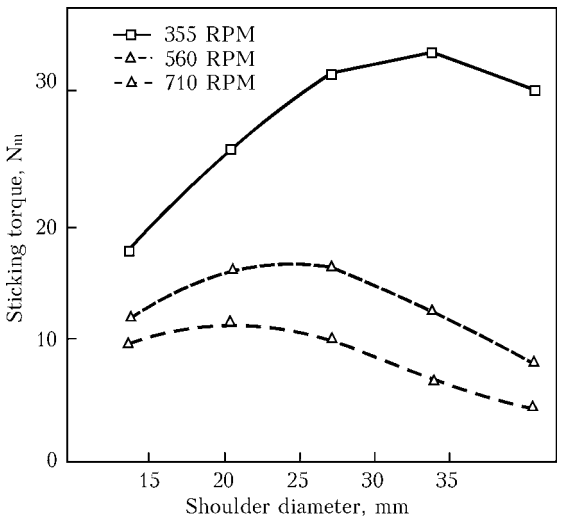

Figure 2. Variation of sticking (M_T) torque with shoulder diameter for FSW of 3.5 mm thick AA7075 at a welding speed of 0.67 mm/s [14]

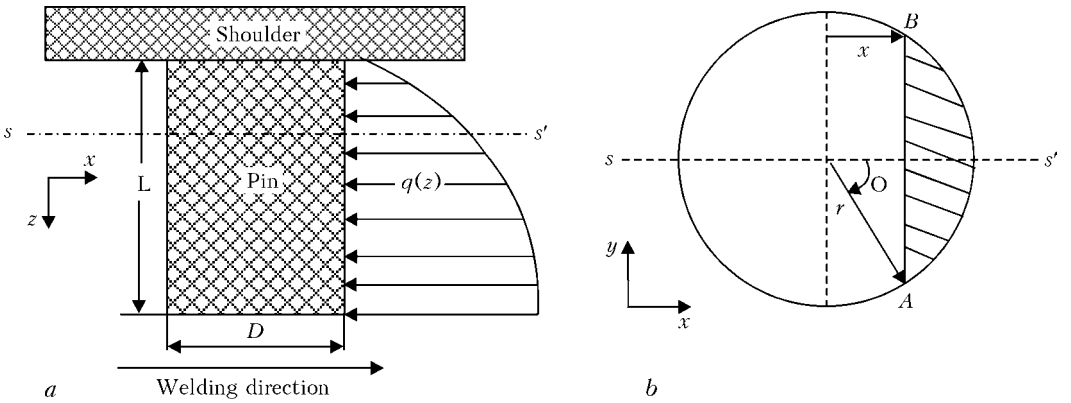

Figure 3. Schematic distribution of force on a typical straight cylindrical tool pin (*a*) and cross-section of pin profile along section S-S.18 (*b*)

nation of torsion due to torque and bending due to traverse force [18, 19].

Figure 3, *a* shows a schematic force distribution, $q(z)$, on a straight cylindrical tool pin in FSW. It can be noted that the force distribution, $q(z)$ would be in adirection opposite to the welding direction. Figure 3, *b* depicts a transverse cross-section of the tool pin along S-S in Figure 3, *a*. The bending moment (M_y) experienced at any point A on the tool pin profile can be estimated as [18]:

$$M_y = \int_{z_1}^{L} zq(z)dz, \tag{4}$$

where L is the length of pin; z_1 is the distance of the point A from the root of the pin; $q(z)$ is the force on an infinitesimal part, dz, of the pin at a distance $(z + z_1)$ from the root of the pin. The normal stress due to bending, σ_B, and the shear stress due to torsion, τ_T, and also due to bending, τ_B, on any point A on the pin profile can be estimated further as [18]

$$\sigma_B = \frac{M_y x}{I_{yy}}, \tag{5}$$

$$\tau_T = \frac{M_T r}{J_z}, \tag{6}$$

and

$$\tau_{TB} = \frac{VQ}{I_{yy} g}, \tag{7}$$

where I_{yy} and J_z are the second moment and polar moment of inertia for the pin structure, respectively; M_y and M_T are the bending moment and sticking torque, respectively; V is the shear force and Q is the first moment of inertia of the section beyond chord AB (in Figure 3, *b*) about the neutral axis; x is the normal distance between the neutral axis and the chord AB; r is the pin radius and g is the length of the chord AB. These components of stresses can be used to compute the resultant maximum shear stress, τ_{max}, experienced by the tool pin as [18]

$$\tau_{max} = \sqrt{\left(\frac{\sigma_B}{2}\right)^2 + (\tau_B + \tau_T \sin\theta)^2 + (\tau_T \cos\theta)^2}. \tag{8}$$

It follows that t_{max} times a safety factor, f, should be lower than the shear strength of the tool material at the prevailing working temperature to avoid premature shear failure of the tool pin in the operating range of process parameters.The pin length depends on the thickness of the work piece. The geometry of the pin must be determined based on its load bearing ability, i.e., the ability to withstand the maximum shear stress.

The traverse force on the pin increases with increase in the pin length as shown in Figure 4. As the plate thickness increases, pins of longer lengths are required. A longer pin experiences higher resultant maximum shear stress and a larger cross-sectional area of the pin becomes necessary to avoid pin failure. However,as the pins of large diameters move forward, plasticized alloys must fill up the void space left behind by large pins. Any disruption of the flow of plasticized material or a small reduction in temperature will enhance the occurrence of defects such as worm-holes.The traverse force on the tool can be measured using a dynamometer, and the values can be used to monitor defect formation during FSW because the large forces indicate sluggish material flow. Thus, the lower limit for the tool pin diameter can be prescribed from the calculation of the maximum shear stress on the tool pin and the upper limit for the pin diameter can be estimated considering the weld quality.

The load bearing abilities of pins with circular, square and triangular cross-sections have been compared [19] under similar welding conditions. For comparison of the three cross-sections, the triangular cross section is considered to be of equilateral shape and thetriangular and the square cross-sections are considered to have dimensions that fit within the circular pin profile. It is found that the lowest and the highest values of the maximum shear stress are experienced by the circular and the triangular pin cross-sections,

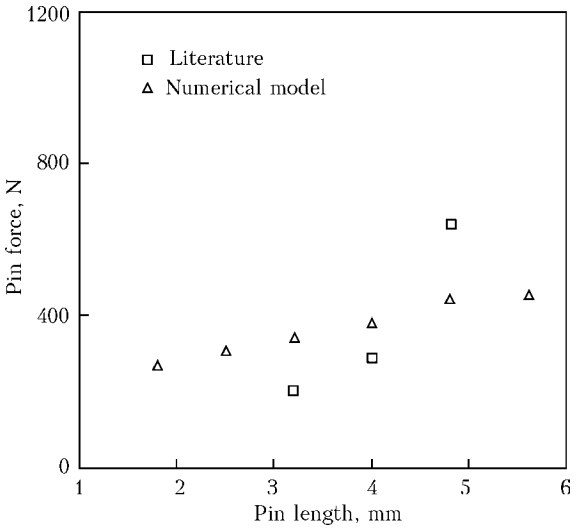

Figure 4. A comparison of computed and corresponding estimated values of traverse force on tool pin in FSW of AA6061 at tool rotational speed of 650 RPM, welding velocity of 3.33 mm/s and pin diameter of 7.6 mm [18, 20]

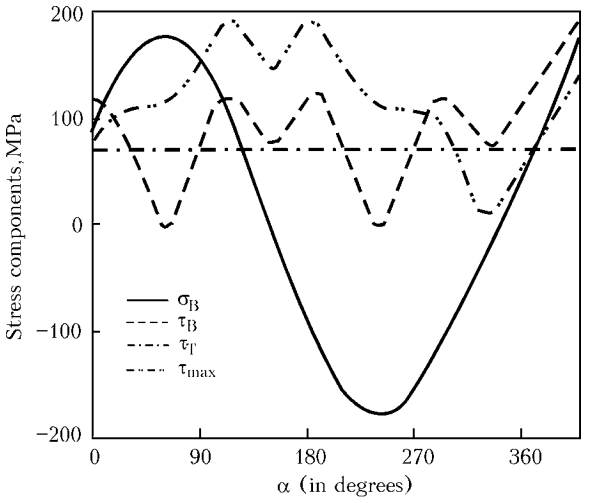

Figure 5. Variation of fluctuating stress components — normal stress for bending, σ_B, shear stress due to bending, τ_B, shear stress due to torsion, τ_T, and the maximum shear stress, τ_{max} for one completerotation of the tool during FSW of AA7075-T6 usingtriangular pin profile [19]

respectively. During one complete rotation, the triangular pin cross-section experiences the largest fluctuation of the maximum shear stressfollowed by the square and the circular pin profiles. Figure 5 shows the typical fluctuation of various stresses during rotation expressed as a function of angle with the welding direction. The large fluctuation of maximum shear stress during rotation makes the triangular cross section susceptible to fatigue failure.

Durabilityof FSW tool. Since the tool pin is structurally the weakest section of FSW tool, itsdegradation due to plastic deformation or wear as well as its ability to withstand the torsion and bending stresses are of significant concern. A review of the currently used and potential tool materials is available in the literature [17]. The material to be used for FSW tool should be cost effective and have high strength, hardness and good toughness, and high melting and softening temperatures [17]. Furthermore, the geometry of the tool pin for a given material should also be assessed for its low susceptibility to premature failure for various values of FSW variables. Recently, a tool durability factor has been proposed that can indicate whether the thermo-mechanical environment experienced by a tool pin for a given FSW condition is safe enough to avoid a premature shear fracture [21, 22]. The tool durability factor does not consider vibration and other

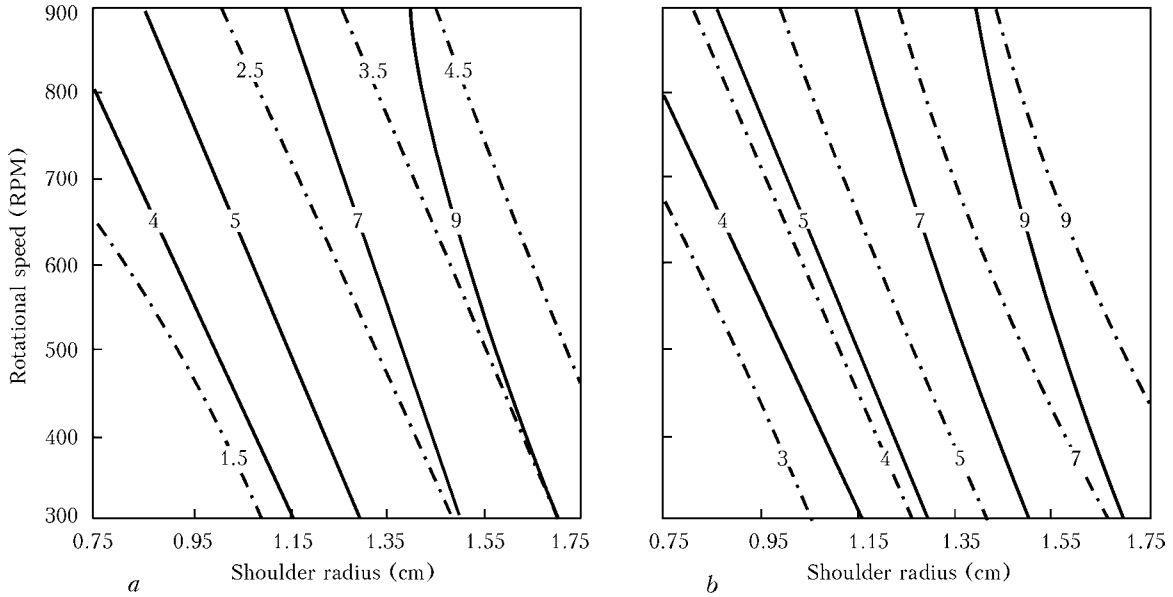

Figure 6. Tool durability indices as function of shoulder radius and rotational speed in FSW of AA 7075 using a tool pin diameter of 4 mm and axial pressure of 18 MPa: *a* — shows the effect of plate thickness with the solid and dashed lines referring to thinner (2.9 mm) and thicker (5.7 mm) plates, respectively, at a welding speed of 1.0 mm/s; *b* — shows the effect of welding speed with the solid and dashed lines depicting the lower (1.0 mm/s) and higher (4.5 mm/s) speeds, respectively for a plate thickness of 2.9 mm [22]

abrupt causes of tool degradation. However, the progressive degradation of the tool pin may be minimized by focusing on the relative severity of maximum shear stress it experiences for various welding conditions. The tool durability factor is defined as the ratio of the shear strength of the tool material at the peak temperature and the resultant maximum shear stress experienced by the tool pin due to bending and torsion.

Figure 6 shows a typical tool durability map for various tool shoulder radius and rotational speed for the FSW AA7075 alloy. A comparison of the solid and dashed lines in Figure 6, *a* shows how the tool durability index or the factor of safety for the tool pin changes with the change in plate thickness. During FSW of thick plates, there is considerable decrease intemperature away from the tool shoulder and the pin encounterscooler and stronger workpiece material near the lower part of the pin. As a result, tools encounter large stresses during welding of thick plates and the tool durability decreases with increase in plate thickness. Similarly, a comparison of the solid and the dashed lines in Figure 6, *b* shows that an increase in welding speed reduces the value of tool durability index. Similarly an increase in the welding speed reduces the rate of heat generation per unit length of weld resulting in relatively colder material around the tool pin. As a result, the tool durability index decreases with increase in welding speed.

Conclusions

Because FSW is a new and complex process, its comprehensive understanding is still developing. Unlike other welding processes, its existing knowledge base cannot be relied upon for solving important contemporary problems such as extending its reach to harder materials such as steels and titanium alloys. Well tested heat transfer and material flow models provide a recourse to address the important issues based on solid scientific principles. The examples reviewed here show how the quantitative understanding of heat transfer and material flow offer new insights about optimizing tool design. Both the optimization of shoulder diameter and the consequences of alternative tool pin shapes can be examined based on well tested numerical models. In the past, the sophisticated numerical models of heat transfer and materials flow in welding have not been widely used in industry.In recent years, the modeling results for FSW have been presented as easy to use process maps,enabling practicing engineers to select welding conditions based on scientific principles to extend tool life. Apart from revelingsignificant insight about the FSW process, the numerical models of heat transfer and materials flow can also providesignificant competitive technological advantage.

1. Mishra, R.S., Ma, Z.Y. (2005) Friction stir welding and processing. *Mater. Sci. Eng. R*, 50(**1/2**), 1–78.
2. Nandan, R., DebRoy, T., Bhadeshia, H.K.D.H. (2008) Recent advances in friction-stir welding — process, weldment structure and properties. *Prog. Mater. Sci.*, 53(**6**), 980–1023.
3. Threadgill, P.L., Leonard, A.J., Shercliff, H.R. et al. (2009) Friction stir welding of aluminum alloys. *Int. Mater. Rev.*, 54(**2**), 49–93.
4. Bhadeshia, H.K.D.H., DebRoy, T. (2009) Critical assessment: friction stir welding of steels. *Sci. Technol. Weld. Joining*, 14(**3**), 193–196.
5. DebRoy, T., Bhadeshia, H.K.D.H. (2010) Friction stir welding of dissimilar alloys — a perspective. *Ibid.*, 15(**4**), 266–270.
6. Heideman, R., Johnson, C., Kou, S. (2010) Metallurgical analysis of Al/Cu friction stir spot welding. *Ibid.*, 15(**7**), 597–604.
7. Nandan, R., Roy, G.G., DebRoy, T. (2006) Numerical simulation of three-dimensional heat transfer and plastic flow during friction stir welding. *Metallurgical and Materials Transact. A*, **37A**, 1247–1259.
8. Nandan, R., Roy, G.G., Lienert, T.J. et al. (2007) Three-dimensional heat and material flow during friction stir welding of mild steel. *Acta Materialia*, **55**, 883–895.
9. Colegrove, P.A., Shercliff, H.R., Zettler, R. (2007) A model for predicting the heat generation and temperature in friction stir welding from the material properties. *Sci. Technol. Weld. Joining*, 12(**4**), 284–297.
10. Nandan, R., Lienert, T.J., DebRoy, T. (2008) Toward reliable calculations of heat and plastic flow during friction stir welding of Ti–6Al–4V alloy. *Int. J. of Materials Research*, 99(**4**), 434–444.
11. Arora, A., Nandan, R., Reynolds, A.P. et al. (2009) Torque, power requirement and stir zone geometry in friction stir welding through modeling and experiments. *Scr. Mater.*, **60**, 13–16.
12. Arora, A., Zhang, Z., De, A. et al. (2009) Strain and strain rates during friction stir welding. *Ibid.*, **61**, 863–866.
13. Arora, A., DebRoy, T., Bhadeshia, H.K.D.H. (2011) Back of the envelope calculations in friction stir welding — velocities, peak temperature, torque, and hardness. *Acta Mater.*, 59(**5**), 2020–2028.
14. Mehta, M., Arora, A., De, A. et al. (2011) Tool geometry for friction stir welding — optimum shoulder diameter. *Metall. Mater. Transact. A*, 42A(**9**), 2716–2722.
15. Arora, A., De, A., DebRoy, T. (2011) Toward optimum friction stir welding tool shoulder diameter. *Scripta Mater.*, 64(**1**), 9–12.
16. Elangovan, K., Balasubramanian, V. (2008) Influences of tool pin profile and tool shoulder diameter on the formation of friction stir processing zone in AA6061 aluminium alloy. *Mater. Des.*, 29(**2**), 362–373.
17. Rai, R., De, A., Bhadeshia, H.K.D.H. et al. (2011) Review: friction stir welding tools. *Sci. Technol. Weld. Joining*, 16(**4**), 325–342.
18. Mehta, M., Arora, A., De, A. et al. (2012) Load bearing capacity of tool pin during friction stir welding. *Int. J. Adv. Manuf. Technol.*, **61**, 911–920.
19. Mehta, M., De, A., DebRoy, T. (2013) Probing load bearing capacity of circular and non-circular tool pins in friction stir welding. In: *Proc. of 9th Int. Conf. on «Trends in Welding Research»* (Chicago, USA, June 04–08, 2012), ASM International, 563–571.
20. Sorensen, C.D., Stahl, A.L. (2007) Experimental measurement of load distribution on friction stir weld pin tools. *Metall. Mater. Transact. B*, **38B**, 451–459.
21. Manvatkar, V.D., Arora, A., De, A. et al. (2012) Neural network models for peak temperature, torque, traverse force, bending stress and maximum shear stress during friction stir welding. *Sci. Technol. Weld. Joining*, 17(**6**), 460–466.
22. DebRoy, T., De, A., Bhadeshia, H.K.D.H. et al. (2012) Tool durability maps for friction stir welding of an aluminum alloy. *Proc. of the Royal Society A*, **468**, 3552–3570.

Received 21.06.2013